

Entanglement Hamiltonian of the quantum Néel state

Didier Poilblanc¹

¹Laboratoire de Physique Théorique, CNRS, UMR 5152 and Université de Toulouse, UPS, F-31062 Toulouse, France
(Dated: September 6, 2022)

I show that a spinon-doped Resonating Valence Bond state gives a qualitative description of the U(1)-symmetric Néel ground state of the spin-1/2 square lattice Heisenberg antiferromagnet. Using a simple $D = 3$ Projected Entangled Pair State representation, I discuss the entanglement properties resulting from a partition of an (infinite) cylinder. In particular, I find that the Entanglement Hamiltonian is (almost exactly) a chain of a dilute mixture of heavy (\downarrow spins) and light (\uparrow spins) hardcore bosons, where light particles are subject to long-range hoppings.

I. INTRODUCTION

It is known from early Quantum Monte Carlo (QMC) simulations that the ground state (GS) of the spin-1/2 Heisenberg antiferromagnet (AFM) on the bipartite square lattice is magnetically ordered [1] and, hence, breaks the hamiltonian SU(2) symmetry. The GS can be viewed as a “quantum Néel state” (QNS) where the maximum classical value $m_{\text{stag}} = 1/2$ of the staggered magnetization is reduced by (moderate) quantum fluctuations. More recent QMC simulations [2] have provided GS energy, staggered magnetization and spin-spin correlations with unprecedented accuracy. In particular, it has been established that the QNS exhibits power-law decaying spin-spin correlations characteristic of a *critical state* [3].

Recently, a number of new powerful tools based on entanglement measures have emerged. The reduced density matrix (RDM) of a bipartioned system provides new insights to the system via the derivation of the entanglement spectrum and its associated Entanglement Hamiltonian (see definitions later). However, subtleties might arise in the entanglement properties of systems with spontaneously broken continuous symmetry, such as the QNS which breaks SU(2) symmetry down to U(1). Recent studies of the entanglement entropy (the entropy associated to the RDM) have revealed anomalous sub-leading corrections [4, 5] to the area law – i.e. the linear scaling of the entropy with the length of the cut. As proposed afterwards, the origin of such corrections may lie in the restoration of the SU(2) symmetry in a finite system [6] where one has a unique GS instead of a degenerate manifold. A priori important differences may occur in the entanglement properties of a Néel GS breaking the continuous SU(2) symmetry explicitly. In particular, one expects the Entanglement Hamiltonian (EH) of a symmetry-broken QNS to differ qualitatively from the one associated to the GS with restored SU(2) symmetry, as e.g. computed for a line-shaped sub-system [7].

I use here a simple Projected Entangled Pair State [8, 9] ansatz to represent the QNS and calculate the EH associated to a bipartition of an infinite cylinder. As shown recently, a EH with local interactions is expected in a gapped bulk phase (with short-range entanglement), whereas a diverging interaction length of the EH is the

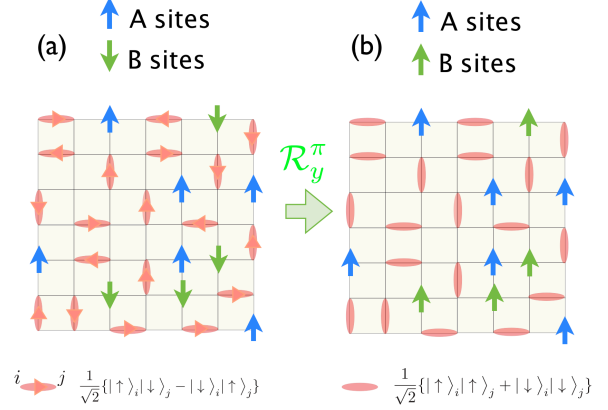


FIG. 1. (a) The Néel state is represented as a spinon-doped RVB state : Singlets are oriented from the A to the B sublattice and doped spinons are polarized along \hat{z} ($-\hat{z}$) on the A (B) sites. Implicitly, a sum over all singlet/spinon configurations is assumed, the average spinon density being controlled by a fugacity. (b) Under a π -rotation around \hat{y} on all the B-sites, all spinons become oriented along \hat{z} and singlets transform into $\frac{1}{\sqrt{2}}\{|\uparrow\uparrow\rangle + |\downarrow\downarrow\rangle\}$ on every NN bonds.

hallmark of critical behavior in the bulk [9]. One therefore expects to see fingerprints of the critical behavior of the QNS in its Entanglement Hamiltonian.

II. DOPED-RVB ANSATZ FOR THE NÉEL STATE

I start with the square lattice Resonating Valence Bond (RVB) wavefunction defined as an equal-weight superposition of nearest-neighbor (NN) hardcore singlet coverings [10, 11]. The sign structure of the wave function is fixed by imposing that the singlets $|\uparrow\downarrow\rangle - |\downarrow\uparrow\rangle$ are all oriented from one A sublattice to the other B sublattice. Such a wave function is a global spin singlet – i.e. a SU(2)-invariant state – with algebraic dimer correlations (and short-range spin correlations) [12, 13]. To construct a simple ansatz for the QNS, let us now assume that one breaks SU(2) symmetry down to U(1) by doping the NN RVB state with on-site spinons (i.e. spin-1/2 excitations) with *opposite* orientations on the two sublattices.

For simplicity, I choose hereafter the staggered magnetization pointing along the \hat{z} -axis. Such a simple ansatz is schematically shown in Fig. 1(a). The average density of spinons – identical on the two sublattices – directly gives the staggered magnetization m_{stag} ($\times 2$) and, as one will see later on, can be controlled by a fugacity γ .

Before going further, it is convenient to rewrite the Néel-RVB state in a translationally invariant form. Indeed, under a (spin) π -rotation around \hat{y} on the B-sites, B-spinons transform as $|\downarrow\rangle \rightarrow |\uparrow\rangle$ and $|\uparrow\rangle \rightarrow -|\downarrow\rangle$. Under such a (unitary) transformation, the new Néel-RVB state acquires the same (average) polarization on the A and B sublattices as shown in Fig. 1(b). The original NN singlets are also transformed into $\frac{1}{\sqrt{2}}\{|\uparrow\uparrow\rangle + |\downarrow\downarrow\rangle\}$ dimers which are now symmetric w.r.t. the bond centers.

III. PEPS CONSTRUCTION AND ENERGETICS

Such a state can in fact be represented by a PEPS $|\Psi_{\text{PEPS}}\rangle$ with bond dimension $D = 3$, where each lattice site is replaced by a rank-5 tensor $\mathcal{A}_{\alpha,\alpha';\beta,\beta'}^s$ labeled by one physical index, $s = 0$ or 1 , and by four virtual bond indices (varying from 0 to 2) along the horizontal (α,α') and vertical (β,β') directions, as shown in Fig. 2(a). Physically, the absence of singlet on a bond is encoded by the virtual index being "2" on that bond. I define :

$$\mathcal{A} = \mathcal{R} + \gamma\mathcal{S}, \quad (1)$$

where \mathcal{R} is the original RVB tensor [14, 15], \mathcal{S} is a polarized spinon tensor and $\gamma \in \mathbb{R}$ is a fugacity controlling the average spinon density. To enforce the hardcore dimer constraint, one takes $\mathcal{R}_{\alpha,\alpha';\beta,\beta'}^s = 1$ whenever three virtual indices equal 2 and the fourth one equals s , and $\mathcal{R}_{\alpha,\alpha';\beta,\beta'}^s = 0$ otherwise. The spinon tensor has only one non-zero element, $\mathcal{S}_{2,2;2,2}^1 = 1$. The wave function amplitudes are then obtained by contracting all virtual indices (except the ones at the boundary of the system). Note that the above PEPS ansatz for the Néel state bares similarities with the one used to describe the honeycomb RVB spin liquid under an applied magnetic field [16]. However, a crucial difference is that this new ansatz is, by construction, fully U(1)-invariant in contrast to the spinon-doped RVB state of Ref. [16].

Following a usual procedure, I now place the square lattice of tensors on infinite cylinders with N_v sites in the periodic (vertical) direction as shown in Fig. 2(b) and use standard techniques (involving exact tensor contractions and iterations of the transfer operator) to compute relevant observables. In the PEPS formulation the boundary conditions B_L and B_R can be simply set by fixing the virtual states on the bonds "sticking out" at each cylinder end. E.g. open boundary conditions are obtained by setting the boundary virtual indices to "2". Generalized

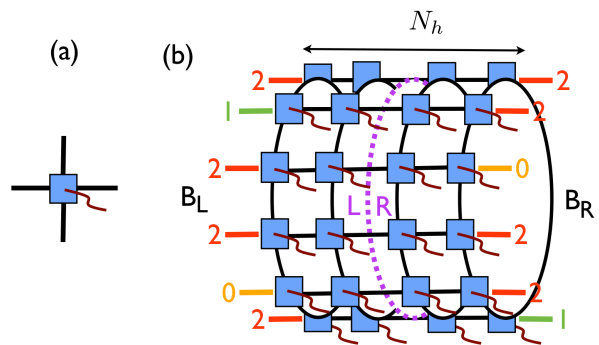


FIG. 2. (Color online) (a) Local (rank-5) PEPS tensor. (b) Tensors are placed on a square lattice wrapped on a cylinder of perimeter N_v and (quasi-) infinite length $N_h \gg N_v$. B_L and B_R boundary conditions are realized by fixing the virtual variables going out of the cylinder ends. A bipartition of the cylinder generates two L and R edges along the cut.

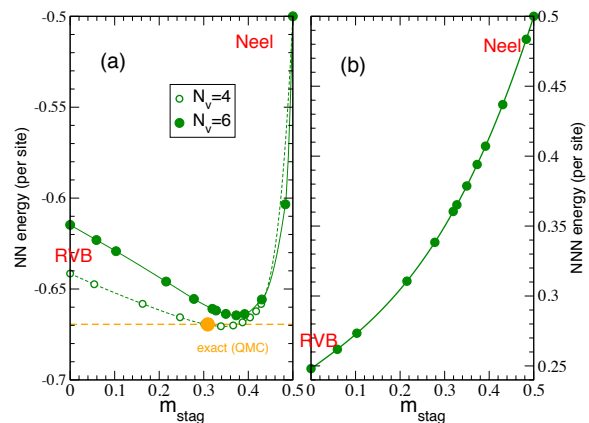


FIG. 3. (Color online) NN (a) and next-NN (b) correlators $2\langle \mathbf{S}_i \cdot \mathbf{S}_j \rangle$ – corresponding to the energies per site in units of the coupling constants – plotted as a function of m_{stag} . Computations are done on infinite cylinders of perimeter $N_v = 4$ and $N_v = 6$.

boundary conditions can be realized as in Fig. 2(b) by setting some of the virtual indices on the ends to "0" or "1".

I have computed the (staggered) magnetization m_{stag} and the expectation values of the spin-1/2 Heisenberg exchange interactions $\mathbf{S}_i \cdot \mathbf{S}_j$ between NN and next-NN sites, varying γ from zero to large values (to approach the classical Néel state). The data (normalized as the energy per site of the corresponding Heisenberg model) are displayed as a function of m_{stag} in Fig. 3(a,b). The NN energy shows a broad minimum around $m_{\text{stag}} \sim 0.35$, a value a bit larger than the QMC extrapolation ~ 0.307 [2] for the pure NN quantum AFM. However, (i) the variational energy curve is rather flat around the minimum and (ii) the minimum energy is only within $\sim 1.5\%$ of

the QMC estimate, a remarkable result considering the simplicity of the one-dimensional family of $D = 3$ PEPS. Note also that the minimum energy agrees very well with fully optimized finite PEPS [18]. I therefore believe that the Néel-RVB state accurately captures the physics of the NN Heisenberg spin-1/2 AFM.

For completeness, I also show the next-NN energy in Fig. 3(b). In fact, the pure RVB state provides the lowest next-NN exchange energy, so that one expects a transition from the Néel state to a RVB state upon increasing the next-NN coupling [19].

IV. ENTANGLEMENT HAMILTONIAN ON INFINITE CYLINDERS

A. Bipartition and reduced density matrix

To define an Entanglement Hamiltonian associated to the family of Néel-RVB wavefunctions, I partition the $N_v \times N_h$ cylinder into two half-cylinders of lengths $N_h/2$, as depicted in Fig. 2(b). Partitioning the cylinder into two half-cylinders reveals two edges L and R along the cut. Ultimately, I aim to take the limit of infinite Néel-RVB cylinders, i.e. $N_h \rightarrow \infty$ as before.

The reduced density matrix of the left half-cylinder obtained by tracing over the degrees of freedom of the right half-cylinder, $\rho_L = \text{Tr}_R\{|\Psi_{\text{PEPS}}\rangle\langle\Psi_{\text{PEPS}}|\}$, can be simply mapped, via a spectrum conserving isometry U , onto an operator σ_b^2 acting only on the $D^{\otimes N_v}$ edge (virtual) degrees of freedom, i.e. $\rho_L = U^\dagger \sigma_b^2 U$ [9]. The *Entanglement (or boundary) Hamiltonian* H_b introduced above is defined as $\sigma_b^2 = \exp(-H_b)$. As σ_b^2 , H_b is one-dimensional and its spectrum – the *entanglement spectrum* (ES) – is the same as the one of $-\ln \rho_A$. Note that the left and the right half-cylinders give identical EH. For further details on the derivation and the procedure, the reader is kindly asked to refer to Ref. 9.

For a topological state, such as the $\gamma = 0$ RVB state, the Entanglement Hamiltonian depends on the choice of the B_L and B_R cylinder boundaries that define “topological sectors” [15, 17]. Adding any staggered magnetization m_{stag} in the PEPS immediately breaks the gauge symmetry of the tensors which is responsible for the disconnected topological sectors, as also happens in the case of field-induced magnetized RVB states [16]. Therefore, all topological sectors are mixed and H_b become independent of the boundary conditions B_L and B_R provided $N_h \rightarrow \infty$. Note also that H_b inherits the $U(1)$ symmetry (associated to rotations around the direction of m_{stag}) of the Néel state.

B. Expansion in terms of N-body operators

To have a better insight of the Entanglement Hamiltonian, I expand it in terms of a basis of N -body operators, $N = 0, 1, 2, \dots$ [9, 15]. For this purpose, I

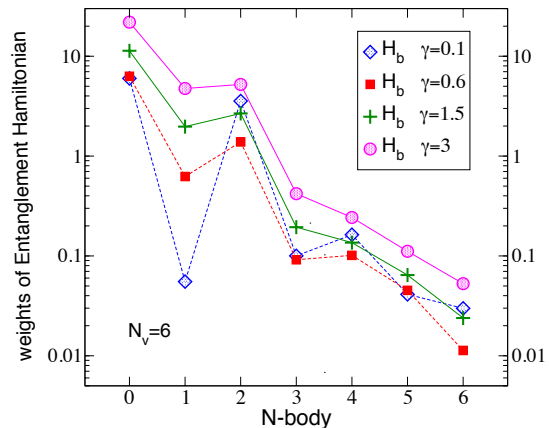


FIG. 4. (Color online) Weights of the Entanglement Hamiltonian H_b expanded in terms of N -body operators. Data of several Néel-RVB wavefunctions (whose γ values are mentioned on the plot) are shown. Calculations are done on an infinite cylinder with perimeter $N_v = 6$. As seen e.g. in Ref. [15], finite size effects for such integrated quantities are typically quite small.

use a local basis of $D^2 = 9$ (normalized) \hat{x}_ν operators, $\nu = 0, \dots, 8$ which act on the local (i.e. at some site i) configurations $\{|0\rangle, |1\rangle, |2\rangle\}$, where $|2\rangle$ is the vacuum or “hole” state and $|0\rangle$ and $|1\rangle$ can be viewed as spin down and spin up particles, respectively. More precisely, $\hat{x}_0 = \mathbb{I}^{\otimes 3}$, $\hat{x}_1 = \sqrt{\frac{3}{2}}(|0\rangle\langle 0| - |1\rangle\langle 1|)$ and $\hat{x}_2 = \frac{1}{\sqrt{2}}(|0\rangle\langle 0| + |1\rangle\langle 1| - 2|2\rangle\langle 2|)$, for the diagonal matrices, complemented by $\hat{x}_3 = \hat{x}_4^\dagger = \sqrt{3}|0\rangle\langle 1|$ acting as (effective) spin-1/2 lowering/raising operators, and $\hat{x}_5 = \hat{x}_7^\dagger = \sqrt{3}|2\rangle\langle 0|$ and $\hat{x}_6 = \hat{x}_8^\dagger = \sqrt{3}|2\rangle\langle 1|$ acting as particle hoppings. In this basis H_b reads [15],

$$H_b = c_0 N_v + \sum_{\nu, i} c_\nu \hat{x}_\nu^i + \sum_{\nu, \mu, r, i} d_{\nu\mu}(r) \hat{x}_\nu^i \hat{x}_\mu^{i+r} + \sum_{\lambda, \mu, \nu, r, r', i} e_{\lambda\mu\nu}(r, r') \hat{x}_\lambda^i \hat{x}_\mu^{i+r} \hat{x}_\nu^{i+r'} + \dots, \quad (2)$$

where site superscript indices have been added and only the first one-body, two-body and three-body terms are shown.

The total weights corresponding to each order of the expansion of H_b in terms of N -body operators are shown in Fig. 4 as a function of the order N using a semi-logarithmic scale. The data reveal clearly a fast decay of the weight with the order N . This decay is compatible with an exponential law although more decades in the variation of the weights (i.e. larger N_v) would be needed to draw a definite conclusion. In any case, H_b is dominated by two-body contributions in addition to the normalization constant and subleading one-body terms. The quantum Néel state is believed to be critical with power-law decay of spin-spin correlations [3]. Therefore,

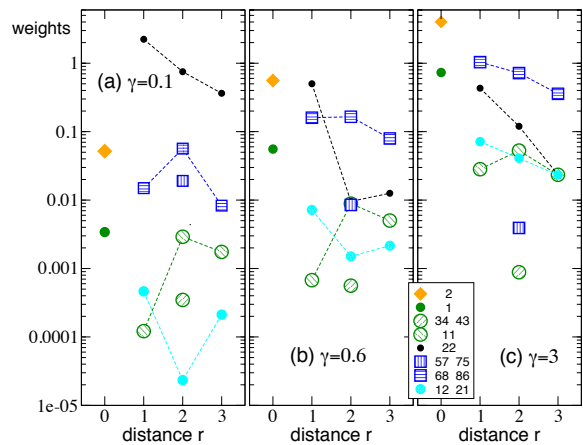


FIG. 5. Largest weights $|c_\nu|$ and $|d_{\nu\mu}(r)|^2$ of the one-body (i.e. $r = 0$) and two-body operators in the expansion of H_b of the Néel-RVB PEPS as a function of distance r , for increasing γ values (corresponding to staggered magnetizations $m_{\text{stag}} \sim 0.059, 0.327$ and 0.483 , respectively).

according to Ref. [9], one expects H_b to be long-ranged to some degree. So, one still needs to refine the analysis and investigate further the r -dependence of the leading two-body contributions. In the next Subsection, I show that H_b indeed possesses long-range two-body terms that I characterize.

C. Entanglement Hamiltonian: an effective one-dimensional t-J model

It is known that the EH of the $\gamma = 0$ RVB PEPS belongs to the $1/2 \oplus 0$ representation of $SU(2)$ and its Hilbert space is the same as the one of a one-dimensional bosonic t-J model [15], interpreting $|0\rangle$ and $|1\rangle$ states ($|2\rangle$ states) as \downarrow and \uparrow spins (holes). In the presence of a finite (staggered) magnetization in the bulk, the $SU(2)$ symmetry is broken but H_b keeps the unbroken $U(1)$ symmetry corresponding to spin rotations around the direction of the staggered magnetization.

The (largest) non-zero real coefficients in (2) computed on an infinitely-long cylinder of perimeter $N_v = 6$ are shown in Fig. 5(a-c) for small (a), intermediate (b) and large (c) (staggered) magnetizations. At large and intermediate values of m_{stag} , one finds a dominant one-body (diagonal) term which can be interpreted as a chemical potential term (up to a multiplicative factor) :

$$\mathcal{H}_2 = c_2 \sum_i \hat{x}_2^i = \frac{3}{\sqrt{2}} c_2 \sum_i (n_i - 2/3), \quad (3)$$

where n_i counts the number of particles (i.e. “0” and “1” states) on site i . The subleading one-body operator takes the form of a Zeeman coupling :

$$\mathcal{H}_1 = \sqrt{6} c_1 \sum_i S_i^z, \quad (4)$$

where S_i^z is an effective spin-1/2 component (along \hat{z}) and $c_1 \simeq c_2/10$.

The leading 2-body contributions are hopping terms at all distances for the majority “spins” ($|1\rangle$ states) :

$$\begin{aligned} \mathcal{H}_{68}(r) &= d_{68}(r) \sum_i (\hat{x}_8^i \hat{x}_6^{i+r} + \hat{x}_6^i \hat{x}_8^{i+r}) \\ &= 3d_{68}(r) \sum_i (b_{i+r,1}^\dagger b_{i,1} + b_{i,1}^\dagger b_{i+r,1}), \end{aligned} \quad (5)$$

where $b_{i,s}^\dagger$ ($b_{i,s}$) are the canonical bosonic creation (annihilation) operators of the virtual $s = 0, 1$ states. Note that the minority spins ($|0\rangle$ states) only hop at even distances (weights at odd distances are negligible) with much weaker amplitudes, $d_{57} = d_{75} \ll d_{68} = d_{86}$. The next subleading corrections are diagonal 2-body density-density interactions

$$\begin{aligned} \mathcal{H}_{22}(r) &= d_{22}(r) \sum_i \hat{x}_2^i \hat{x}_2^{i+r} \\ &= \frac{9}{2} d_{22}(r) \sum_i (n_i - 2/3)(n_{i+r} - 2/3), \end{aligned} \quad (6)$$

which become dominant when $\gamma, m_{\text{stag}} \rightarrow 0$.

Other generic operators allowed by the $U(1)$ symmetry, like the anisotropic XXZ chain ($d_{11} \neq d_{34} = d_{43}$) or mixed operators of the form $\mathcal{H}_{12} \propto \sum_i S_i^z (n_{i\pm r} - 2/3)$ are also present but their amplitudes turn out to be quite small. Interestingly, H_b (approximately) conserves the hole “2-charge” and, hence, does not contain pair-field operators with sizable amplitudes, in contrast to previous studies of $D = 3$ PEPS [15, 16]. If one restricts to the dominant contributions (3) and (5), H_b is exactly a chain of a dilute mixture of heavy (\downarrow spins or $|0\rangle$ states) and light (\uparrow spins or $|1\rangle$ states) hardcore bosons, where light particles are subject to long-range hopping.

V. ENTANGLEMENT SPECTRUM

For completeness, I now investigate the Entanglement Spectrum. By definition the ES is the spectrum of $-\ln \rho_L$. Since ρ_L and $\sigma_b^2 = \exp(-H_b)$ are related by an isometry, it is also the spectrum of the Entanglement Hamiltonian H_b . ES are shown in Fig. 6(a-c) for 3 values of the fugacity γ , as a function of the momentum along the cut. Since σ_b^2 conserves the total S_z of the chain ($U(1)$ symmetry), it can be block-diagonalized using this quantum number and the eigenvalues of $-\ln \sigma_b^2$ are displayed in each S_z sector separately. It can be seen from Fig. 6(a) that the $\gamma = 0$ $SU(2)$ spin multiplets are split by a small spinon density. For increasing γ (i.e. staggered magnetization), the splittings of the Kramer’s multiplets increase (see Fig. 6(b,c)) due to the relative increase of the amplitudes of the $SU(2)$ -symmetry breaking terms like (5) in the EH. In the limit of large γ where the classical Néel state is approached, one finds separated bands of energy levels. It may be that the ES is gapped for all γ

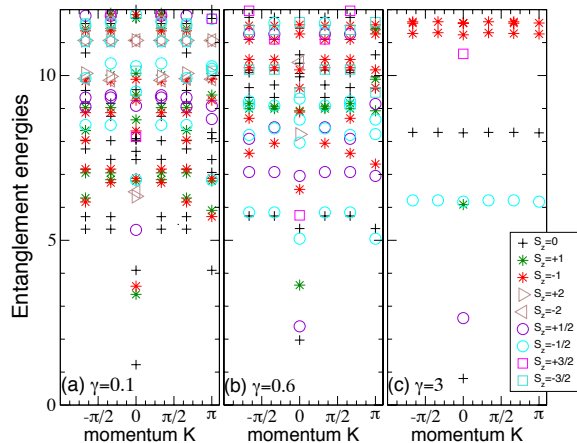


FIG. 6. Entanglement spectrum of a bipartitioned $N_v = 6$ RVB-Néel cylinder as a function of the momentum along the cut, for different values of the spinon fugacity $\gamma = 0.1, 0.6$ and 3 corresponding to $m_{\text{stag}} \sim 0.059, 0.327$ and 0.483 , respectively. Different symbols are used for different S_z sectors of the edge.

but finite size effects remain too small to reach a definite conclusion.

VI. SUMMARY AND DISCUSSION

In this paper, I have investigated entanglement properties of a simple one-dimensional family of PEPS designed to describe qualitatively the GS of the square lat-

tice AFM. These ansätze exhibit a finite staggered magnetization i.e. they break explicitly the $SU(2)$ symmetry down to $U(1)$ and can be studied on infinite cylinders with a finite perimeter. Hence, differences in the entanglement measures may occur compared to (e.g. QMC) studies where symmetry is restored in a finite system. Thanks to the PEPS structure, the Entanglement Hamiltonian associated to a bipartition of the cylinder can be derived exactly (for a fixed perimeter). The EH inherits the $U(1)$ symmetry of the Néel state and possesses a very simple structure : (i) its Hilbert space is the same as the one of a one-dimensional bosonic t - J model, interpreting the 3 virtual states on the edge as a \uparrow spin, a \downarrow spin and a hole, (ii) when expanded using a local basis of operators, it shows dominant two-body interactions and (iii) higher-order operators (three-body terms and beyond) represent less than 10% of its total weight. Examining in details the form of the two-body interactions, I find that the dominant ones are long-range hoppings of the majority (let say \uparrow) spins. It is plausible that this form of EH gives rise to subleading corrections to the area law of the entanglement entropy. It would be interesting to test this scenario in QMC by pinning the staggered magnetic order with a small external (staggered) field, taking the limit of infinite system size first.

I acknowledge fundings by the “Agence Nationale de la Recherche” under grant No. ANR 2010 BLANC 0406-0 and support from the CALMIP supercomputer center (Toulouse). I thank Claire for her patience and I am indebted to Fabien Alet, Ignacio Cirac, Nicolas Laflorencie, Roger Melko, Anders Sandvik, Norbert Schuch and Frank Verstraete for numerous discussions and insightful comments.

-
- [1] J. D. Reger and A. P. Young, *Monte Carlo Simulations of the Spin-1/2 Heisenberg Antiferromagnet on a Square Lattice*, Phys. Rev. B **37**, 5978 (1988).
 - [2] A. W. Sandvik and H. G. Evertz, *Loop updates for variational and projector quantum Monte Carlo simulations in the valence-bond basis*, Phys. Rev. B **82**, 024407 (2010).
 - [3] A. W. Sandvik, *Lecture notes for course given at the 14th Training Course in Physics of Strongly Correlated Systems, Salerno (Vietri sul Mare), Italy, in October 2009*, AIP Conf.Proc. 1297:135 (2010).
 - [4] A. B. Kallin, M. B. Hastings, R. G. Melko, and R. R. P. Singh, *Anomalies in the entanglement properties of the square-lattice Heisenberg model*, Phys. Rev. B **84**, 165134 (2011).
 - [5] Hyejin Ju, A. B. Kallin, P. Fendley, M. B. Hastings, and R. G. Melko, *Entanglement scaling in two-dimensional gapless systems*, Phys. Rev. B **85**, 165121 (2012).
 - [6] M. A. Metlitski and T. Grover, *Entanglement Entropy of Systems with Spontaneously Broken Continuous Symmetry*, arXiv:1112.5166 (2011).
 - [7] D. J. Luitz, N. Laflorencie, and F. Alet, *Participation spectroscopy and entanglement Hamiltonian of quantum spin models*, arXiv:1404.3717 (2014).
 - [8] N. Schuch, M. M. Wolf, F. Verstraete, and J. I. Cirac, *Computational Complexity of Projected Entangled Pair States*, Phys. Rev. Lett. **98**, 140506 (2007).
 - [9] J. I. Cirac, D. Poilblanc, N. Schuch, and F. Verstraete, *Entanglement spectrum and boundary theories with projected entangled-pair states*, Phys. Rev. B **83**, 245134 (2011).
 - [10] P. W. Anderson, *Resonating valence bonds: A new kind of insulator?*, Mat. Res. Bull. **8**, 153 (1973).
 - [11] P. W. Anderson, *The resonating valence bond state in La_2CuO_4 and superconductivity*, Science **235**, 1196 (1987).
 - [12] A. F. Albuquerque and F. Alet, *Critical correlations for short-range valence-bond wavefunctions on the square lattice*, Phys. Rev. B **82**, 180408R (2010).
 - [13] Y. Tang, A. W. Sandvik and C. L. Henley, *Properties of resonating valence bond spin liquids and critical dimer models*, Phys. Rev. B **84**, 174427 (2011).
 - [14] N. Schuch, D. Poilblanc, J. I. Cirac and D. Perez-Garcia, *Resonating valence bond states in the PEPS formalism*, Phys. Rev. B **86**, 115108 (2012).
 - [15] D. Poilblanc, N. Schuch, D. Perez-Garcia and J. I. Cirac, *Topological and entanglement properties of resonating va-*

- lence bond wave functions, Phys. Rev. B **86**, 014404 (2012).
- [16] D. Poilblanc, N. Schuch, and J. I. Cirac, *Field-induced superfluids and Bose liquids in Projected Entangled Pair States*, Phys. Rev. B **88**, 144414 (2013).
- [17] N. Schuch, D. Poilblanc, J. I. Cirac and D. Perez-Garcia, *Topological order in PEPS: Transfer operator and boundary Hamiltonians*, Phys. Rev. Lett. **111**, 090501 (2012).
- [18] M. Lubasch, J. I. Cirac, and M.-C. Bañuls, *Algorithms for finite Projected Entangled Pair States*, arXiv:1405.3259 (2014).
- [19] Ling Wang, Didier Poilblanc, Zheng-Cheng Gu Xiao-Gang Wen and Frank Verstraete, *Constructing gapless spin liquid state for the spin-1/2 J1-J2 Heisenberg model on a square lattice*, Phys. Rev. Lett. **111**, 037202 (2013).